International Immunopharmacology 161 (2025) 115055

Contents lists available at ScienceDirect

International Immunopharmacology

journal homepage: www.elsevier.com/locate/intimp

Acetyl zingerone inhibits chondrocyte pyroptosis and alleviates osteoarthritis progression by promoting mitophagy through the PINK1/parkin signaling pathway

Zhuangzhuang Zhang [a,1], Tianyue Huang [b,1], Xu Chen [c], Jie Chen [a], Hang Yuan [d], Ning Yi [e], Chunbao Miao [f], Rongbin Sun [a,*], Su Ni [a,*]

[a] Department of Orthopedics, The Third Affiliated Hospital of Nanjing Medical University, Changzhou Second People's Hospital, Changzhou Medical Center, Changzhou, Jiangsu 213003, PR China
[b] The Third Affiliated Hospital of Nanjing Medical University, Changzhou Second People's Hospital, Changzhou Medical Center, Changzhou, Jiangsu 213003, PR China
[c] Department of Orthopaedics, The Third People's Hospital of Changzhou, Changzhou, Jiangsu, 213000, PR China
[d] Department of Joint Surgery, Quzhou People's Hospital, Quzhou, Zhejiang, 324000, PR China
[e] Department of Orthopedics, Panjin Central Hospital, 124000, PR China
[f] Jiangsu Key Laboratory of Advanced Catalytic Materials and Technology, Jiangsu Province Key Laboratory of Fine Petrochemical Engineering, School of Petrochemical Engineering, Changzhou University, Changzhou, Jiangsu 213164, PR China

ARTICLE INFO

Editor: Dr. Yongchun Shen

Keywords:
Acetyl zingerone
Osteoarthritis
Mitophagy
NLRP3 inflammasome
Pyroptosis

ABSTRACT

Osteoarthritis (OA) is a common chronic degenerative joint disease, characterized by osteophyte formation and cartilage degeneration. A growing number of studies have found that nod-like receptor pyrin domain 3 (NLRP3) inflammasome-mediated chondrocyte pyroptosis plays a crucial role in the development of OA. Acetyl zingerone (AZ) is a small molecule compound, chemically synthesized to retain the key functional properties of curcumin and zingerone, while exhibiting enhanced anti-inflammatory, antioxidant, and anti-aging effects. Previous studies in our group have found an inhibitory effect on ferroptosis in AZ osteoarthritis. However, its specific mechanism of action has not been fully explained. Therefore, we further delved into whether AZ could alleviate OA in mice by affecting mitophagy and pyroptosis. In an in vitro study, we observed that AZ alleviated LPS + ATP-induced pyroptosis in chondrocytes and inhibited the activation of the NLRP3 inflammasome, a key factor in pyroptosis. Moreover, by using the mitophagy activators Resveratrol, the autophagy lysosome inhibitor chloroquine (CQ) and siPINK1 to knock down PINK1, we demonstrated that AZ promoted PINK1/Parkin-mediated mitophagy. AZ enhanced PINK1/Parkin-mediated mitophagy, facilitating the clearance of damaged mitochondria, thereby reducing reactive oxygen species (ROS) production and suppressing NLRP3 inflammasome activation. This cascade mitigated chondrocyte pyroptosis and promoted collagen synthesis. Moreover, AZ demonstrated a comparable pro-regenerative effect on the extracellular matrix to that observed with the standard osteoarthritis treatment, rapamycin. In animal experiments, intra-articular administration of AZ similarly promoted mitophagy and inhibited chondrocyte pyroptosis, alleviating osteoid formation and cartilage damage. Collectively, these findings suggest that AZ may mitigate OA progression by activating mitophagy and attenuating pyroptosis, highlighting its potential as a preventive therapeutic approach for OA.

1. Introduction

Osteoarthritis (OA) is a degenerative joint disease primarily affecting middle-aged and older adults, and is the leading cause of joint pain and disability. OA significantly impacts patients' quality of life and imposes a substantial economic burden worldwide [1]. It is characterized by articular cartilage erosion, subchondral bone degeneration, bone spur formation, and chronic synovial inflammation [2]. Additionally, an

* Corresponding author at: Department of Orthopedics, The Third Affiliated Hospital of Nanjing Medical University, Changzhou Second People's Hospital, Changzhou Medical Center, 68 Ge Hu Middle Road, Changzhou, Jiangsu 213003, PR China.
E-mail addresses: sunrongbin@njmu.edu.cn (R. Sun), nisu@njmu.edu.cn (S. Ni).
[1] The authors contributed equally to the research.

https://doi.org/10.1016/j.intimp.2025.115055
Received 24 February 2025; Received in revised form 19 May 2025; Accepted 4 June 2025

imbalance between the synthesis and degradation of the cartilage extracellular matrix (ECM) plays a crucial role in the loss and destruction of articular cartilage [3]. Currently, the main treatments for OA are analgesics and nonsteroidal anti-inflammatory drugs (NSAIDs), which provide only temporary pain relief and are associated with various adverse effects [4,5]. Therefore, discovering a drug that can alleviate, prevent, or even reverse the progression of OA is of utmost importance. Recently, traditional herbs and derivatives of traditional medicines have shown promise in alleviating osteoarthritis with minimal side effects, offering the added benefits of being affordable and widely available [6,7].

Pyroptosis is a novel form of programmed cell death characterized by inflammasome activation, which is dependent on caspase-1 and accompanied by the release of large amounts of pro-inflammatory cytokines, such as IL-1β and IL-18 [8]. The inflammasome is associated with various inflammatory diseases, including inflammatory bowel disease, Parkinson's disease, and osteoarthritis [9–11]. The most well-known of these is the NLRP3 inflammasome, a protein complex composed of NLRP3, apoptosis-associated speck-like protein (ASC), and the cysteine protease caspase-1 [12]. The NLRP3 inflammasome is activated by factors such as pathogen-associated molecular patterns (PAMPs) like lipopolysaccharide (LPS), microbes, and viruses, as well as damage-associated molecular patterns (DAMPs) such as extracellular ATP, uric acid, and cholesterol crystals. Upon activation, the NLRP3 inflammasome assembles and cleaves pro-caspase-1 into active caspase-1, which in turn cleaves the pro-inflammatory cytokines pro-IL-1β and pro-IL-18, converting them into their active forms, IL-1β and IL-18 [13,14]. Concurrently, the NLRP3 inflammasome triggers pyroptosis by initiating the cleavage of gasdermin D (GSDMD), leading to the formation of pores in the cell membrane [15]. Recent studies suggest that NLRP3 inflammasome activation plays a central role in the pathogenesis of osteoarthritis. Chao Lou et al. found that Cucurbitacin B inhibited NLRP3 inflammasome activation and pyroptosis, thereby slowing the progression of OA [16]. Thus, blocking NLRP3 inflammasome activation represents an effective therapeutic strategy for the treatment of osteoarthritis.

Mitochondria play a critical role in energy production, reactive oxygen species (ROS) generation, and the regulation of apoptosis [17]. When mitochondria are damaged, they not only become inefficient at energy production but also tend to over-accumulate ROS, which exacerbates chondrocyte damage [18]. Mitophagy, a selective form of autophagy, is essential for maintaining mitochondrial mass and ROS homeostasis, serving to eliminate dysfunctional mitochondria [19]. Research has demonstrated that mitophagy significantly influences the progression of osteoarthritis [20]. Wei Li et al. found that Forsythoside A inhibited NLRP3 inflammasome activation by promoting mitophagy, which in turn mitigated osteoarthritis and inhibited chondrocyte senescence [21]. The PTEN-induced PINK1/Parkin pathway, recognized as the most extensively studied ubiquitin-dependent pathway for mitophagy, enhances the regulation of mitochondrial quality [22]. Furthermore, damaged mitochondria not only struggle to produce energy effectively but also tend to produce excessive ROS, resulting in the activation of the NLRP3 inflammasome [23]. Based on these findings, we hypothesize that activating PINK1/Parkin-mediated mitophagy could represent a promising therapeutic strategy for addressing chondrocyte pyroptosis and the onset of osteoarthritis.

Lipopolysaccharide (LPS), an outer membrane component of Gram-negative bacteria, is a potent activator of monocytes and macrophages, stimulating the secretion of a variety of pro-inflammatory molecules, including cytokines, nitric oxide (NO), tumor necrosis factor-alpha (TNF-α), and interleukins (such as IL-1 and IL-6), all of which contribute to the onset and progression of inflammatory diseases and cancer [24]. NLRP3 is a core component of the inflammasome, containing a nucleotide-binding oligomerization domain (NACHT) essential for autooligomerization and ATPase activity [25]. Recent studies suggest that LPS and ATP may activate common pathways, such as ROS production, to initiate NLRP3 inflammasome activation, leading to caspase-1-dependent pyroptosis [26,27]. LPS treatment has been shown to reduce chondrocyte proliferation, an effect further exacerbated by ATP treatment, while also increasing the expression of pyroptosis-related proteins, including chondrocyte caspase-1, cleaved caspase-1, and GSDMD-N [28]. Furthermore, LPS- and ATP-induced mitochondrial dysfunction activates NLRP3 inflammasomes through mitochondrial damage-associated molecular patterns (mtDAMPs), which impair mitochondrial membrane potential and promote the release of mitochondrial ROS [29,30]. Therefore, mitochondrial dysfunction plays a central role in the activation of NLRP3 inflammasomes via multiple mechanisms [31]. Consequently, strategies aimed at inhibiting NLRP3 inflammasome activation and pyroptosis by maintaining mitochondrial homeostasis and promoting mitophagy may offer promising therapeutic avenues for the treatment of inflammatory diseases.

Acetyl zingerone (AZ) is a small molecule compound derived from the natural structures of curcumin and zingerone, with chemical modifications to enhance the structure of curcumin. It retains the key functional properties of both curcumin and zingerone while exhibiting more pronounced anti-inflammatory, antioxidant, and anti-aging effects. Additionally, AZ improves solubility, photostability, and absorption [32]. Previous studies have shown that AZ protects skin melanocytes from UV-induced damage, promotes collagen synthesis, and inhibits matrix metalloproteinase production [33,34]. Our team has also demonstrated that AZ possesses strong antioxidant properties and can slow the progression of osteoarthritis in mice [35]. However, the specific mechanisms underlying AZ's effects remain incompletely understood. The relationship between curcumin and mitophagy has recently been reported in a variety of diseases [36,37], and Acetyl curcumin is structurally alike to curcumin. Therefore, it is reasonable to hypothesize that mitophagy plays an important role in the treatment of OA with AZ. In this study, we utilized ATDC5 chondrocytes to establish an in vitro model of pyroptosis, examining the effects of AZ on chondrocyte activity, mitochondrial damage, extracellular matrix synthesis and degradation, mitophagy, and pyroptosis. Furthermore, we established a mouse OA model to confirm the therapeutic effects of AZ through indicators such as cartilage histology, changes in mitophagy, and expression of pyroptosis proteins. Our results suggest that AZ exhibits significant anti-OA activity, primarily due to its antioxidant properties, enhancement of mitophagy, and suppression of pyroptosis. These findings have important clinical implications.

2. Materials and methods

2.1. Materials and reagents

Acetyl zingerone (AZ) was synthesized in the laboratory of Dr. Miao at Changzhou University. Lipopolysaccharides (LPS, L3129), Adenosine 5′-triphosphate disodium salt hydrate (ATP, A6419) and chloroquine (CQ, C6628) were purchased from Merck (Missouri, USA). Resveratrol (HY-16561) and Rapamycin (AY-22989) were obtained from MedChemExpress™ (Monmouth Junction, NJ, USA). The LDH Cytotoxicity Assay Kit (C0016), Reactive Oxygen Species Assay Kit (S0033S), Annexin V-FITC Apoptosis Detection Kit (C1062S), BeyoClick™ EdU Cell Proliferation Kit with AF488 (C0071S) and Mito-Tracker Green (C1048) were sourced from Beyotime (Shanghai, China). The Cell Counting Kit-8 (U10014A) was purchased from UU-bio (Suzhou, China). The MT-1 MitoMP Detection Kit (MT13) and MitoBright IM Red for Immunostaining (MT15) were obtained from Dojindo™ (Beijing, China). The stubRFP-sensGFP-LC3 Lentivirus (GPL2001A) was sourced from Genechem™. jetPRIME® Transfection Reagent (101000046) was sourced from Polyplus (Shanghai, China). MitoSOX™ Red, Alexa Fluor 488, Alexa Fluor 596 and ProLong™ Diamond Antifade Mountant with DAPI (P36962) were purchased from Thermo Fisher™ (Shanghai, China). The mouse cell line ATDC5 (ZQ0938) was obtained from

Shanghai Zhongqiao Xinzhou Biological Technology Co., Ltd. (Shanghai, China). DMEM/F-12 medium and fetal bovine serum (FBS) were acquired from Gibco™ (California, USA). The following western blot antibodies were purchased from Abclonal™ (Wuhan, China): β-Actin (AC038), ASC (A1170), GSDMD (A20197), p62 (A19700), LC3B (A19665), Collagen II (A19308), Aggrecan (A12045), MMP3 (A11418), and MMP13 (A11148). Parkin (BD-PT3593) was purchased from Biodragon™ (Suzhou, China), IL-1β (P10749) from Servicebio (Wuhan, China), NLRP3 (15101S) from Cell Signaling™. Caspase-1 was sourced from Santa Cruz Biotechnology™ (sc-398,715). PINK1 (23274–1-AP) and MMP13 (18165–1-AP) were obtained from Proteintech™ (Wuhan, China). All other materials and reagents were of analytical grade.

2.2. Ethics statemen

The procedures for the care and use of animals were approved by the Institutional Animal Care and Use Committee (the file number is IACUC-2407014). Mice were housed at the Wutai Animal Facility of Nanjing Medical University, and the experiments were conducted by experimenters who hold the animal experiment certificate of the Animal Core Facility of Nanjing Medical University.

2.3. Animals and treatments

Twenty-eight male, 8-week-old C57BL/6 J mice were purchased and all procedures were performed in accordance with internationally recognized ethical guidelines. The mice were housed under standard conditions (temperature 22–24 °C, humidity 45–55 %, 12-h light-dark cycle, with free access to food and water). After one week of acclimatization, medial meniscus destabilization (DMM) was performed to shear the medial meniscus ligament of the right knee, following previous literature, resulting in medial meniscus instability and inducing OA lesions. One week after surgery, the animals were divided into four groups ($n = 7$): Sham group, DMM group, DMM + Resveratrol (50 mg/kg) treatment group, and DMM + AZ (1 mg/kg) treatment group. Intra-articular injections into the knee joint were administered using insulin needles twice a week for a duration of 8 weeks. Mice in the Sham and DMM groups received 10 μL of carrier solution (30 % PEG300, 5 % DMSO, and deionized water), while the DMM + resveratrol and DMM + AZ treatment groups were each injected with 10 μL of either resveratrol at a dose of 50 mg/kg or AZ at a dose of 1 mg/kg, respectively.

2.4. Cell culture

The ATDC5 cell line was purchased from Zhong Qiao Xin Zhou Biotechnology (Shanghai, China). ATDC5 cells were cultured in DMEM/F12 (G4612, Servicebio) under standard conditions, with 10 % fetal bovine serum (FBS, Gibco, USA) and 1 % penicillin/streptomycin (Gibco, USA), at 37 °C with 5 % carbon dioxide (CO_2). Chondrocytes with good growth status after four generations were selected for the experiment. The culture medium was changed every two days.

2.5. Cell viability analysis

ATDC5 chondrocytes were inoculated in 96-well plates at a density of 1×10^4 cells per well. The cells were co-treated with different concentrations of AZ (25, 50, 100, and 200 μM, dissolved in DMSO) and 5 μg/mL LPS + 2 μM ATP for 24 h and 48 h; controls were cultured in medium containing 1/1000 DMSO. The medium was changed once a day. Subsequently, cells were incubated with fresh complete medium containing 10 μL CCK-8 reagent for 2 h at 37 °C. Complete medium containing CCK-8 reagent without cells and untreated cells were used as blank and mock controls, respectively. Absorbance (OD) at 450 nm was detected using a microplate reader (Epoch, Bio-Tek Instruments, USA).

2.6. EdU assays

Chondrocytes were cultured in confocal dishes and treated with 5 μg/mL LPS + 2 μM ATP, with or without various concentrations of AZ (25, 50, 100, or 200 μM; dissolved in DMSO) for 24 h. Cell proliferation was then assessed using the BeyoClick™ EdU Cell Proliferation Kit with AF555, following the manufacturer's instructions. Briefly, EdU (20 μM) was added to the culture medium and incubated at 37 °C for 2 h. After incubation, cells were fixed with 4 % paraformaldehyde for 15 min and permeabilized with 0.3 % Triton X-100 for 10 min at room temperature. Following three washes with the provided washing solution, cells were incubated for 30 min at room temperature in the dark with the Click Reaction Solution, composed of 430 μL Click Reaction Buffer, 20 μL $CuSO_4$, 1 μL Azide 555, and 50 μL Click Additive Solution per sample. Cells were then counterstained with 1× Hoechst 33342 for 10 min at room temperature, protected from light, followed by three washes (3–5 min each). Fluorescence imaging was performed using a laser scanning confocal microscope (CLSM-900, Carl Zeiss, Oberkochen, Germany). Quantitative analysis was conducted using ImageJ software.

2.7. LDH release

Cytotoxicity was measured by colorimetric determination of lactate dehydrogenase (LDH) release from cell supernatants using the LDH Cytotoxicity Assay Kit (Beyotime, Shanghai, China), following the manufacturer's instructions.

2.8. Transmission electron microscopy (TEM)

To observe the mitochondria, ATDC5 cells were fixed in 2.5 % glutaraldehyde for 4 h at 25 °C and centrifuged at 800 rpm for 5 min to obtain cell clusters the size of mung beans. The cell clusters were embedded in 1 % agarose and rinsed with 0.1 M phosphoric acid buffer (pH 7.4). Next, 1 % osmium tetroxide (OSO_4) was added to gently lift and suspend the cell clusters. The clusters were then dehydrated, embedded in resin, and stained using uranium-lead double staining (2 % uranyl acetate in saturated alcohol solution protected from light for 8 min and 2.6 %lead citrate protected from carbon dioxide for 8 min). The sections were dried overnight at 25 °C. Cell morphology and subcellular structures were observed using a Hitachi 7800 TEM (Tokyo, Japan).

2.9. Flow cytometry assay

Cell apoptosis was measured with the Annexin V-FITC/PI Apoptosis Detection Kit (Vazyme, Nanjing, China). The cell culture of each well was aspirated into a 5 mL centrifuge tube, the adherent cells were washed twice with PBS, the cells were digested with EDTA-free trypsin, and centrifuged for 5 min at 1800 rpm (300 ×g), 4 °C, the supernatant was discarded, the cells were collected, and the cells were gently resuspended with PBS and counted. After cell resuspension, 100 μL of 1 × Binding Buffer was added and gently blown to a single-cell suspension. Add 5 μL Annexin V-FITC and 5 μL PI Staining Solution, gently blow well, and incubate for 10 min away from light and at room temperature (20–25 °C). Finally, add 400 μL 1 × Binding Buffer and gently mix well. The stained samples were detected by flow cytometry within 1 h. The results were measured using a FACSCalibur flow cytometer (BD Biosciences), and the data were analyzed using FlowJo software.

2.10. Intracellular and mitochondrial ROS detection

ROS levels were measured using DCFH-DA. ATDC5 cells pretreated with or without AZ (100 μM) or CQ (50 μM), was induced with 5 μg/mL LPS + 2 μM ATP for 24 h. The cells were then incubated with 10 μM DCFH-DA for 20 min at 37 °C, washed three times with serum-free medium, and the fluorescence intensity was observed using a Laser Scanning Confocal Microscopy (CLSM-900, Carl Zeiss, Oberkochen,

Germany), with images captured. Quantitative analysis was performed using ImageJ software.

Mitochondrial ROS (mtROS) levels were measured using MitoSOX. Briefly, ATDC5 cells were pretreated with or without Resveratrol (25 μM), AZ (100 μM), and CQ (50 μM), and then induced with 5 μg/mL LPS + 2 μM ATP for 24 h. The cells were incubated with 4 nM MitoSOX for 30 min, washed three times with serum-free medium, and the fluorescence intensity was observed using a Laser Scanning Confocal Microscopy (CLSM-900, Carl Zeiss, Oberkochen, Germany), with images captured. Quantitative analysis was performed using ImageJ software.

2.11. Detection of mitochondrial membrane potential (Δψm)

ATDC5 cells were seeded in confocal dishes at a density of 5×10^5 cells per well and cultured overnight. The following day, the supernatant was removed, and the MT-1 staining working solution from the MT-1 MitoMP Detection Kit (MT13, Dojindo, Shanghai, China) was added. The cells were then incubated at 37 °C for 30 min. Afterward, the medium was removed, and the cells were washed twice with HBSS. Following 24 h of 5 μg/mL LPS + 2 μM ATP and drug treatment, the cells were washed twice with HBSS, and Imaging Buffer solution was added. Finally, the cells were observed using a Laser Scanning Confocal Microscopy (CLSM-900, Carl Zeiss, Oberkochen, Germany). Quantitative analysis was performed using ImageJ software.

2.12. mRFP-GFP-LC3 adenovirus double label assay

P4 generation chondrocytes were seeded into 12-well plates at 50 % fusion. stubRFP-sensGFP-LC3 lentivirus (MOI = 100; Genechem, Shanghai, China) was used to transfect the chondrocytes in 50 % volume of medium for 24 h. In an inverted fluorescence microscope (CX41-32RFL, Olympus, Tokyo, Japan), the successful transfection was observed. The successfully transfected chondrocytes were seeded in confocal petri dishes, and the ATDC5 cells were pretreated with (or without) AZ (100 μM), Res (25 μM) and CQ (50 μM), and induced by 5 μg/mL LPS + 2 μM ATP for 24 h. Finally, the cells were observed by Laser Scanning Confocal Microscopy (CLSM-900, Carl Zeiss, Oberkochen, Germany).

2.13. PINK1 siRNA transfection

PINK1-siRNA (Saisuofei Biotechnology, Wuxi, China) was used to knock down PINK1 in ATDC5 cells, according to the manufacturer's instructions. In addition, ATDC5 cells transfected with non-silencing scrambled siRNA (siNC, Saisuofei Biotechnology. Wuxi, China) were used as the Ctrl. The respective siRNA senses and antisense sequences for PINK1 and Ctrl siRNA were as follows: siPINK1, 5′-GGCAGGUUCCUCCAGCGAATT-3′ and 5′-UUCGCUGGAGGAACCUGCCTT-3′, and siNC, 5′-UUCUCCGAACGUGUCACGUTT-3′ and 5′-ACGUGACACGUUCGGAGAATT-3′. After the cells were successfully transfected, the cells were treated according to the method shown in Section 2.14 and then subjected to Western blot analysis.

2.14. Western blotting analysis

Briefly, ATDC5 cells were pretreated with or without Resveratrol (25 μM), AZ (100 μM), CQ (50 μM), or Rapamycin (100 nM) and then induced with 5 μg/mL LPS + 2 μM ATP for 24 h. Total proteins were extracted from ATDC5 cells and lysed using RIPA buffer (Beyotime, China). Protein concentration was determined using the BCA protein assay kit (P0010S, Beyotime™, Shanghai, China). Protein samples were separated by SDS-PAGE and transferred to PVDF membranes (Millipore, Bedford, USA). The membranes were then blocked in TBST solution containing 5 % non-fat milk for 1 h at room temperature. After blocking, the membranes were incubated overnight at 4 °C with primary antibodies: NLRP3 (1:1000), ASC (1:1000), GSDMD (1:500), Caspase-1 (1:500), IL-1β (1:500), PINK1 (1:500), Parkin (1:1000), p62 (1:1000), LC3B (1:500), Collagen II (1:1000), Aggrecan (1:500), MMP3 (1:1000), MMP13 (1:1000), and β-actin (1:2000). After rinse with TBST three times, the membranes were incubated with HRP-conjugated secondary antibodies (1:5000 dilution) at room temperature for 1 h. Finally, protein bands were detected using an enhanced chemiluminescence kit (ECL kit, BioRad, USA), and densitometric analysis was performed using ImageJ software.

2.15. Micro-CT analysis

After a 2-day formalin fixation, the knee samples were scanned using a high-resolution micro–computed tomography (CT) scanner (Bruker) at 50 kV and 450 mA. The high-resolution micro-CT scans were acquired at a 9-mm voxel size with 360°rotation. Then, 3-dimensional reconstruction was conducted using CTVox software (Bruker). The subchondral trabecular bone of the tibial plateau was defined as the region of interest. The following parameters were measured: (1) Bone volume/tissue volume (BV/TV, %), (2) trabecular thickness (Tb.Th, mm) as a parameter of bone resorption.

2.16. Immunofluorescence (IF)

ATDC5 cells were cultured in confocal dishes for 24 h. After treatment with 5 μg/mL LPS + 2 μM ATP and drugs for an additional 24 h, the cells were fixed with 4 % paraformaldehyde for 15 min, permeabilized with 0.1 % Triton X-100 for 10 min, and blocked with 5 % bovine serum albumin for 1 h. The cells were incubated overnight at 4 °C with primary antibodies against NLRP3, ASC, caspase-1, GSDMD, PINK1, Parkin, p62, LC3B, Collagen II, Aggrecan, MMP3, and MMP13. After washing three times with PBS, the cells were incubated with Alexa Fluor 488 or Alexa Fluor 596 (Thermo Fisher™, Shanghai, China) secondary antibodies for 5 min at room temperature in the dark. The cells were then incubated with DAPI for 1 h at room temperature. To label mitochondria, Mito-Bright IM Red for Immunostaining (1 μM) was added to live ATDC5 cells and incubated at 37 °C for 30 min, followed by fixation with 4 % paraformaldehyde. Further incubated with Parkin and LC3B antibodies overnight at 4 °C. After incubation with Alexa Fluor 596 and DAPI in the dark, fluorescence signals from the region of interest were captured using Laser Scanning Confocal Microscopy (CLSM-900, Carl Zeiss, Oberkochen, Germany). Immunofluorescence intensity was quantified using ImageJ software.

2.17. Histopathological

After mice were euthanized, the knee joints were excised and fixed in 10 % neutral formalin. The tissue was then immersed in 10 % ethylenediaminetetraacetic acid (EDTA), embedded in paraffin, and cut into 5 μm thick sections. Sections were stained with HE and Safranin-O according to the manufacturer's recommendations to visualize grossly morphologic lesions on the tibial plateau. Osteoarthritis Research Society International (OARSI) was used to evaluate knee joint lesions.

2.18. IHC analysis

Immunohistochemical analysis was performed following the instruction of the manufacturer. Paraffin sections were deparaffinized with xylene, rehydrated with ethanol, and washed with PBS. Antigen retrieval was performed by incubating the sections with hyaluronidase at 37 °C for 70 min, followed by treatment with *Streptomyces griseus* protease at room temperature for 10 min, and then washed with PBS. After incubation with H_2O_2 for 10 min and washing with PBS, the sections were incubated overnight at 4 °C in a wet box with primary antibodies against NLRP3 (1:100), LC3B (1:200), Parkin (1:50), MMP13 (1:100), and Collagen II (1:200). On the second day, the sections were incubated with HRP-conjugated secondary antibody for 1 h at room

temperature. Antigen-positive cells were visualized using a DAB substrate kit, and images were captured using light microscopy. Staining intensity was quantified by calculating the area of optical density (AOD) in three different fields of view for each sample using ImageJ software.

2.19. Statistical analysis

All experiments were performed at least three times. Data are presented as mean ± standard deviation and were analyzed or plotted using GraphPad Prism 9.5. Differences between group means were assessed with one-way ANOVA. A p-value of <0.05 was considered statistically significant.

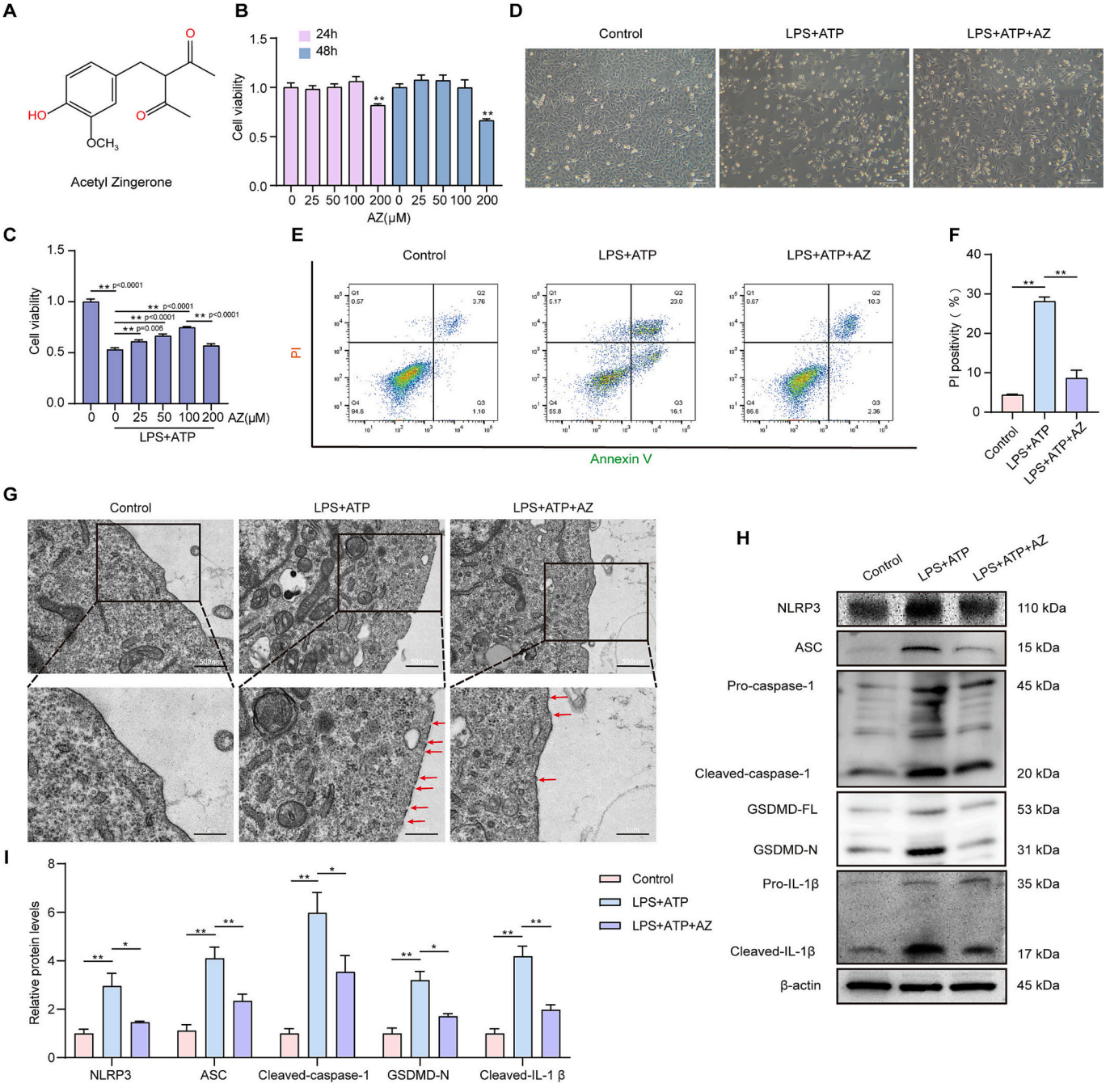

Fig. 1. AZ attenuates LPS-induced pyroptosis in chondrocytes in vitro. (A) Molecular formula of Acetyl Zingerone. (B—C) Chondrocytes viability was assessed using the CCK-8 assay ($n = 3$).(D) Bright-field images of chondrocytes induced by LPS + ATP with or without AZ pretreatment. Scale bar = 100 μm (n = 3). (E, F) Annexin V-FITC/PI staining was performed to detect pyroptosis by flow cytometry, with quantification (n = 3). (G) TEM images of chondrocytes (upper panel, Scale bar = 500 nm; lower panel, Scale bar = 1 μm). Control cells exhibited intact cell membranes with cytoplasmic protrusions. LPS + ATP-treated cells displayed smooth membranes with pores (red arrow). AZ treatment reduced the rupture of cell membranes and pore formation (n = 3). (H, I) Western blot analysis and ImageJ quantification of key pyroptosis proteins, including NLRP3, ASC, Cleaved-caspase-1, GSDMD-N, and Cleaved-IL-1β (n = 3). Data are expressed as mean ± SD. ns, not significant; *$p < 0.05$, and **$p < 0.01$, compared to the corresponding control. (For interpretation of the references to colour in this figure legend, the reader is referred to the web version of this article.)

3. Results

3.1. In vitro, AZ attenuates LPS-induced Pyroptosis in chondrocytes

The structural formula of AZ is shown in Fig. 1A. To identify the optimal concentration for intervention, we assessed the effects of AZ on chondrocyte viability across a range of concentrations (0, 25, 50, 100, and 200 μM) and time points (24 and 48 h) utilizing the CCK-8 assay. The findings indicated that concentrations of AZ below 100 μM did not exhibit cytotoxic effects, while a concentration of 200 μM significantly diminished cell viability (Fig. 1B). Consistent with previous research, treatment with LPS + ATP considerably reduced cell viability. Notably, the CCK-8 assay demonstrated that co-culturing with AZ for 24 h effectively mitigated the cytotoxic effects induced by LPS + ATP, with 100 μM AZ resulting in the most pronounced enhancement of cell viability (Fig. 1C). EdU results showed that LPS + ATP inhibited chondrocyte proliferation, but AZ reversed this inhibition and was most effective at 100 μM (Supplementary Fig. 1. A-B). Consequently, 100 μM AZ was determined to be the optimal concentration for further experimentation.

LPS stimulation activated the NLRP3 inflammasome, inducing pyroptosis through GSDMD-mediated pore formation and interleukin-1β (IL-1β) release, contributing to an inflammatory microenvironment. Microscopic observation revealed that LPS + ATP significantly induced pyroptosis compared to the control, while AZ treatment reversed this effect (Fig. 1D). We utilized flow cytometry to assess propidium iodide (PI) ratios and employed transmission electron microscopy to investigate cell membrane perforation, which serves as an indicator of pyroptosis. Flow cytometry showed that LPS + ATP treatment increased the PI ratio, which was significantly reduced by AZ (Fig. 1E, F). Transmission electron microscopy (TEM) confirmed that AZ preserved membrane integrity by inhibiting LPS + ATP-induced rupture and pore formation (Fig. 1G). We performed Western blot analysis to detect the expression levels of proteins associated with pyroptosis. It was observed that AZ reversed the upregulation of NLRP3 and ASC induced by LPS + ATP. Additionally, AZ inhibited the expression of Cleaved-caspase-1, GSDMD-N, and Cleaved-IL-1β (Fig. 1H, I). These findings suggest that AZ inhibits LPS + ATP-induced pyroptosis in chondrocytes in vitro.

3.2. AZ reduces mtROS production and alleviates mitochondrial damage in LPS-induced chondrocytes

Changes in mitochondrial morphology and function are associated with the pathogenesis of osteoarthritis [38]. Impaired mitochondria not only fail to produce energy efficiently but also excessively accumulate mtROS, which exacerbates chondrocyte damage [39]. It was found that mitochondrial dysfunction acts upstream of NLRP3 activation by ROS to trigger NLRP3 oligomerization or by inducing α-tubulin acetylation to relocate mitochondria to the vicinity of NLRP3 [29]. To evaluate chondrocyte mitochondrial function, we measured levels of ROS (Fig. 2A, B), mtROS (Fig. 2C, D), and Δψm (Fig. 2E, F). After induction with LPS + ATP, the levels of ROS and mtROS in chondrocytes were elevated, while Δψm levels were decreased. These changes suggest that chondrocyte mitochondria are damaged and dysfunctional. However, we found that AZ reversed the LPS + ATP-induced impairment of mitochondrial function in chondrocytes. TEM was utilized to examine mitochondrial morphology. The results showed that control mitochondria exhibited normal, regular and complete morphology. In contrast, mitochondria in chondrocytes treated with LPS + ATP exhibited swelling, vacuolation, reduced density, and structural incompleteness. However, the supplementation of AZ resulted in a notable improvement in mitochondrial morphology, suggesting a potential restorative effect (Fig. 2G). These results suggest that AZ reduces mtROS production and attenuates mitochondrial damage in LPS-induced chondrocytes.

3.3. AZ enhances mitophagy to reduce mitochondrial damage in LPS-induced chondrocytes

Mitophagy is a critical quality control mechanism for mitochondria, with PINK1/Parkin-mediated mitophagy playing a pivotal role in the elimination of dysfunctional mitochondria. This process mitigates the activation of inflammasome and upholds cellular homeostasis [40]. It has been found that the antioxidant Curcumin can rescue impaired mitochondrial function through the induction of mitophagy [36]. This prompts us to hypothesize whether AZ may also exhibit a similar effect as Curcumin. To investigate this, we conducted a series of experiments aimed at verifying the impact of AZ on mitochondrial function and To investigate this, we conducted a series of experiments aimed at verifying the impact of AZ on mitochondrial function and autophagy. TEM was further used to assay mitophagy. The results demonstrated that the addition of AZ significantly improved mitochondrial structure and promoted mitophagy in LPS + ATP-induced chondrocytes (Fig. 2G). The index expression of mitophagy (PINK1, Parkin, P62, LC3II) in chondrocytes was determined by Western blotting. The results demonstrated that AZ treatment significantly increased the expression of PINK1, Parkin, and LC3II, while concurrently decreasing p62 expression. These changes indicate that AZ effectively activates mitophagy in chondrocytes (Fig. 3A, B). Additionally, to further elucidate the role of AZ in the prevention of osteoarthritis associated with mitophagy we investigated the effect of AZ on mitophagy in the presence of the lysosomal inhibitor CQ. CQ inhibits autophagic activity and lysosomal function by blocking lysosomal acidification. IF staining showed that the lysosomal inhibitor CQ suppressed AZ-enhanced mitophagy activity (decreased levels of PINK1, Parkin, and increased levels of P62, LC3B) (Fig. 3C). Finally, we assessed mitochondrial function and showed that CQ also inhibited ROS and mtROS production in AZ-reduced chondrocytes (Fig. 3D-G). These results suggested that AZ increased mitophagy, improved mitochondrial function, and inhibited mtROS generation in LPS + ATP-induced chondrocytes.

3.4. AZ promotes mitophagy and suppresses pyroptosis in LPS-induced chondrocytes through the PINK1/parkin signaling pathway

NLRP3-mediated pyroptosis may exacerbate osteoarthritis by promoting inflammation and damaging cartilage tissues [11]. Mitophagy plays a crucial role in inhibiting NLRP3 activation, thereby mitigating the inflammatory responses associated with osteoarthritis [21]. We further investigated whether AZ the promote mitophagy is linked to pyroptosis. Resveratrol (Res) has been found to activate mitophagy stimulation in a variety of diseases, including arthritis, kidney injury, and lung injury [41–43]. Weimin Fan et al. found that Resveratrol alleviated gouty arthritis by promoting mitophagy to inhibit the activation of NLRP3 inflammation [41]. Western blotting was performed to analyze the expression levels of mitophagy-related proteins PINK1, Parkin, P62, and LC3B. The findings revealed that, compared to the LPS + ATP group, both the AZ and Res groups significantly increased the expression levels of PINK1, Parkin, and the LC3-II/LC3-I ratio in chondrocytes, while simultaneously decreasing the protein expression level of P62. Conversely, the CQ group appeared to attenuate these effects (Fig. 4A, B). These results were further substantiated by immunofluorescence assays, which demonstrated that treatments with AZ and Res significantly enhanced the co-localization of Parkin with mitochondria (Fig. 4C, D), as well as promoted the aggregation of LC3B-labeled autophagosomes toward the mitochondria (Fig. 4E). Additionally, autophagic flux assays revealed that AZ and Res significantly increased the formation of autolysosome (Fig. 4F). Finally, we evaluated mitochondrial function and morphology and found that both AZ and Res significantly reduced mtROS production in chondrocytes (Fig. 4G, H), while also enhancing mitochondrial structure and promoting mitophagy (Fig. 4I). Conversely, the presence of CQ attenuated the effects of AZ, indicating that CQ's inhibition of lysosomal function disrupted the

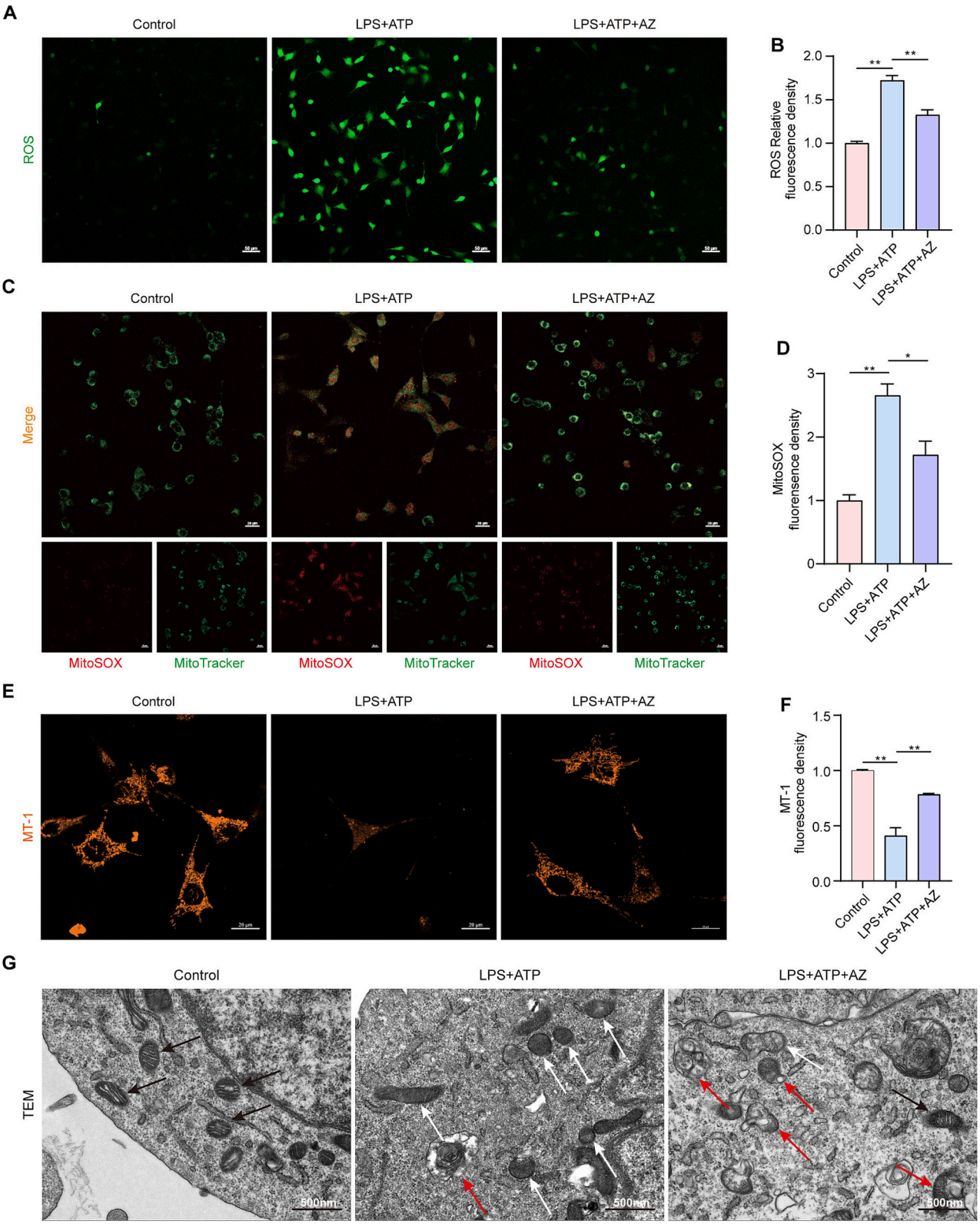

Fig. 2. AZ reduces mtROS production and alleviates mitochondrial damage in LPS-induced chondrocytes. (A, C) ROS and mtROS levels in chondrocytes; (B, D) semi-quantitative analysis of ROS and mtROS fluorescence images. ROS: Scale bar = 100 μm, mtROS: Scale bar = 20 μm (n = 3). (E) Mitochondrial membrane potential in chondrocytes detected by the MT-1 method; (F) semi-quantitative analysis of MT-1 fluorescence images, Scale bar = 20 μm (n = 3). (G) Detection of mitochondrial morphology and mitophagy by TEM, and normal mitochondria (black arrow), damaged mitochondria (white arrow), autophagosomes with mitochondrial-like organelles (red arrow), Scale bar = 500 nm (n = 3). Data are expressed as mean ± SD. ns, not significant; *$p < 0.05$, and **$p < 0.01$, compared with the corresponding control. (For interpretation of the references to colour in this figure legend, the reader is referred to the web version of this article.)

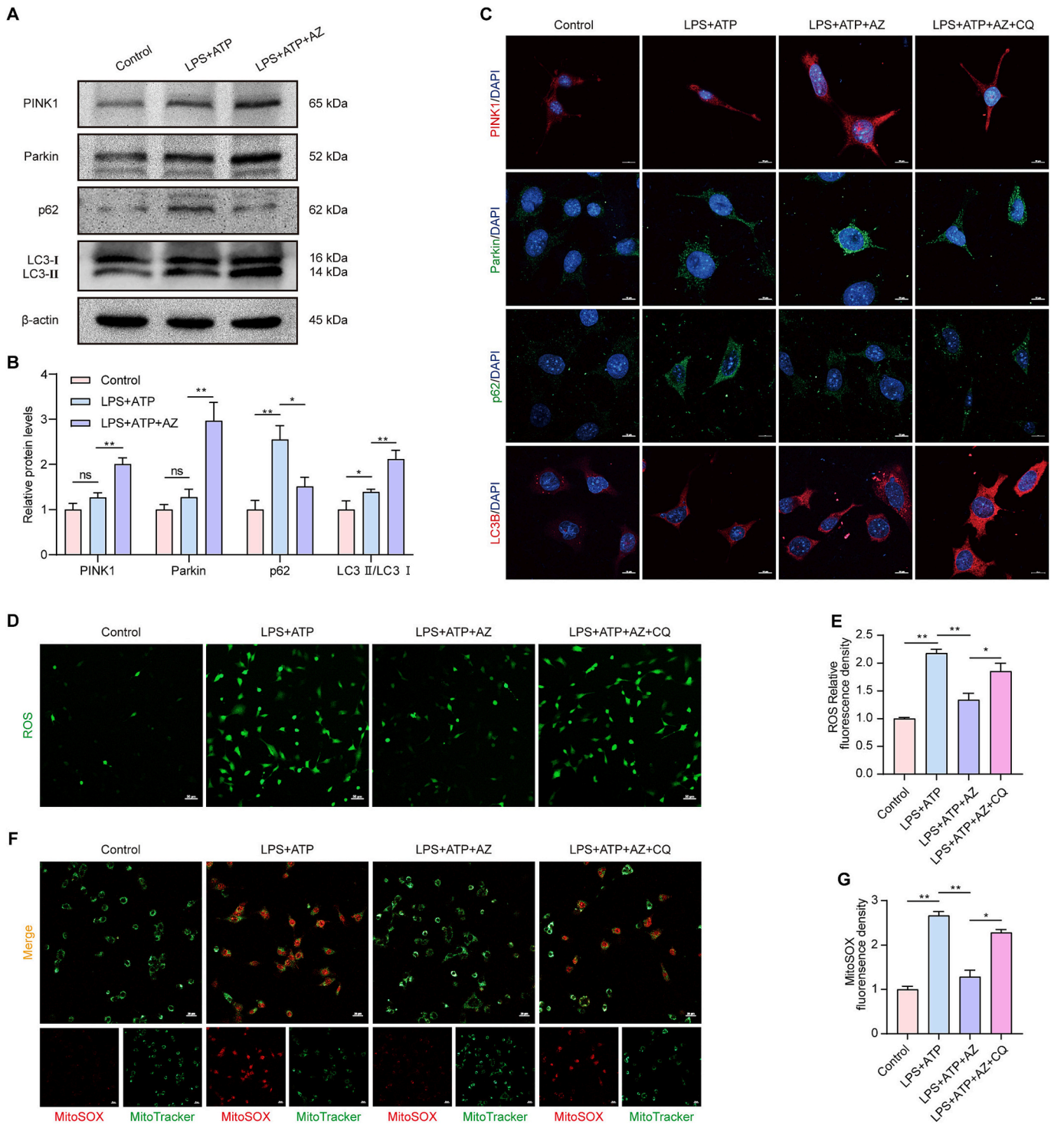

Fig. 3. AZ enhances mitophagy to reduce mitochondrial damage in LPS-induced chondrocytes. (A, B) Detection and quantification of PINK1, Parkin, LC3II, and p62 protein expression through Western blot and ImageJ analysis (n = 3). (C) Immunofluorescence images and quantitative analysis of PINK1, Parkin, p62, and LC3B expression in chondrocytes from the indicated groups. Scale bar = 10 μm (n = 3). (D, F) ROS and mtROS levels in chondrocytes. (E, G) Semi-quantitative analysis of ROS and mtROS fluorescence images. ROS: Scale bar = 100 μm, mtROS: Scale bar = 20 μm (n = 3). Data are expressed as mean ± SD. ns, not significant; $*p < 0.05$, and $**p < 0.01$, compared with the corresponding control.

enhancement of mitophagy activity that AZ typically promotes. These results suggest that AZ, similar to Res, promotes mitophagy by modulating the PINK1/Parkin signaling pathway.

As anticipated, Western blot and immunofluorescence analyses demonstrated that treatment with AZ and Res significantly reduced the expression levels of pyroptosis-associated proteins, including NLRP3, ASC, cleaved-caspase-1, GSDMD-N, and cleaved IL-1β, compared to the LPS + ATP group. In contrast, treatment with CQ inhibited the AZ-induced reduction in the expression of these pyroptosis-related proteins (Fig. 5A-D). Flow cytometry (Fig. 5E, F) and LDH (Fig. 5G) assays further corroborated that both AZ and Res significantly inhibited LPS + ATP-induced chondrocyte pyroptosis. To further elucidate the role of AZ in promoting mitophagy via the PINK1/Parkin signaling pathway, we conducted reverse validation experiments utilizing siRNA to knock

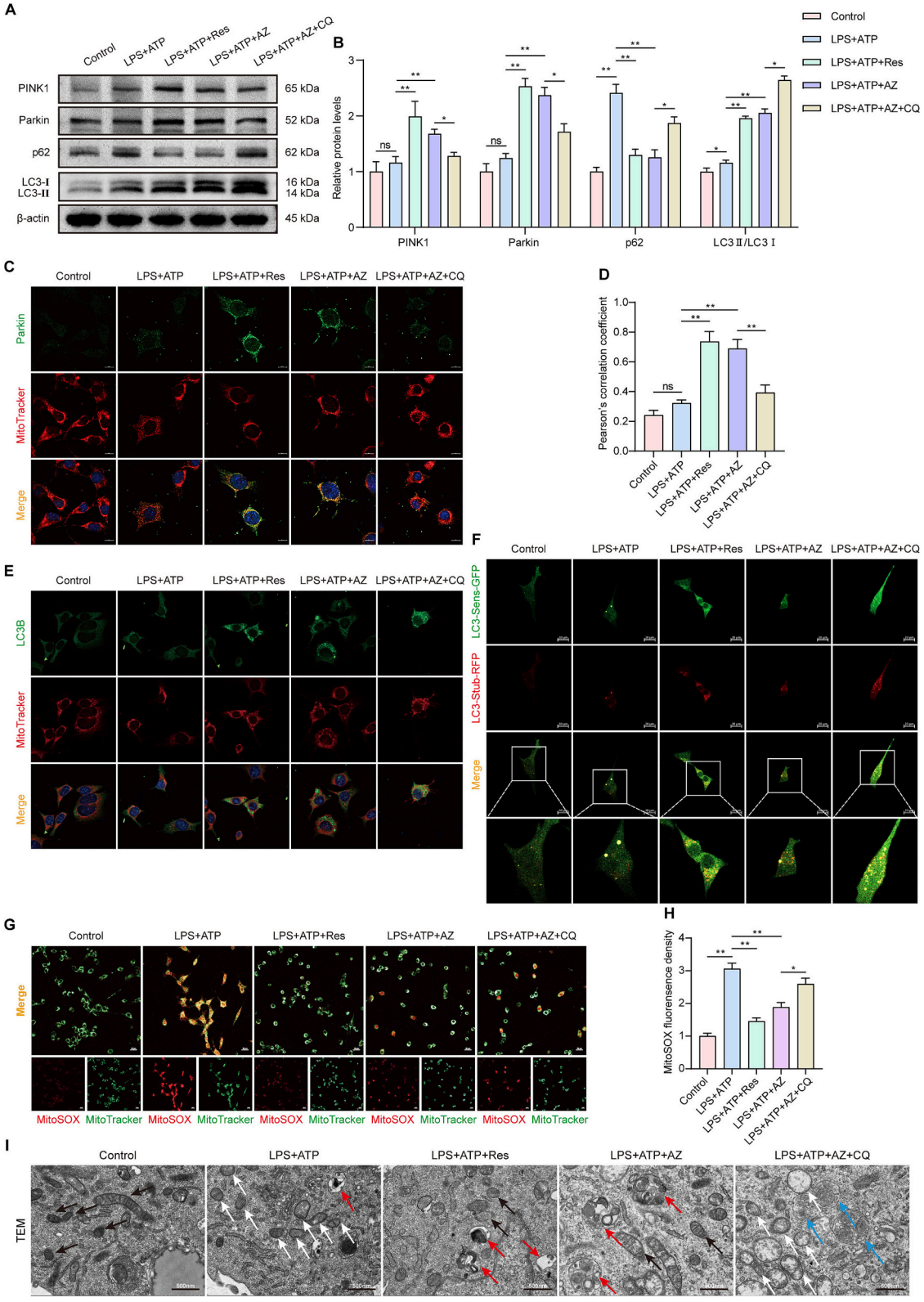

Fig. 4. AZ promotes mitophagy in LPS-induced chondrocytes through the PINK1/Parkin signaling pathway. (A, B) Detection and quantification of PINK1, Parkin, p62, and LC3II protein expression by Western blotting and ImageJ analysis (n = 3). (C, D) Representative images and quantification of immunofluorescence double-labelling of Parkin and MitoTracker. Scale bar = 10 μm (n = 3). (E) Representative images of immunofluorescence double-labelling of LC3B and MitoTracker. Scale bar = 10 μm (n = 3). (F) Chondrocytes transfection with stubRFP-sensGFP-LC3 lentivirus, images acquired by confocal microscopy. Scale bar = 20 μm (n = 3). (G) mtROS levels in chondrocytes. (H) Semi-quantitative analysis of mROS fluorescence images. Scale bar = 20 μm (n = 3). (I) Detection of mitochondrial morphology and mitophagy by TEM, and normal mitochondria (black arrow), damaged mitochondria (white arrow), autophagosomes with mitochondrial-like organelles (red arrow), autophagosomes (blue arrow), Scale bar = 500 nm (n = 3). Data are expressed as mean ± SD. ns: not significant, $*p < 0.05$, and $**p < 0.01$, compared with the corresponding control. (For interpretation of the references to colour in this figure legend, the reader is referred to the web version of this article.)

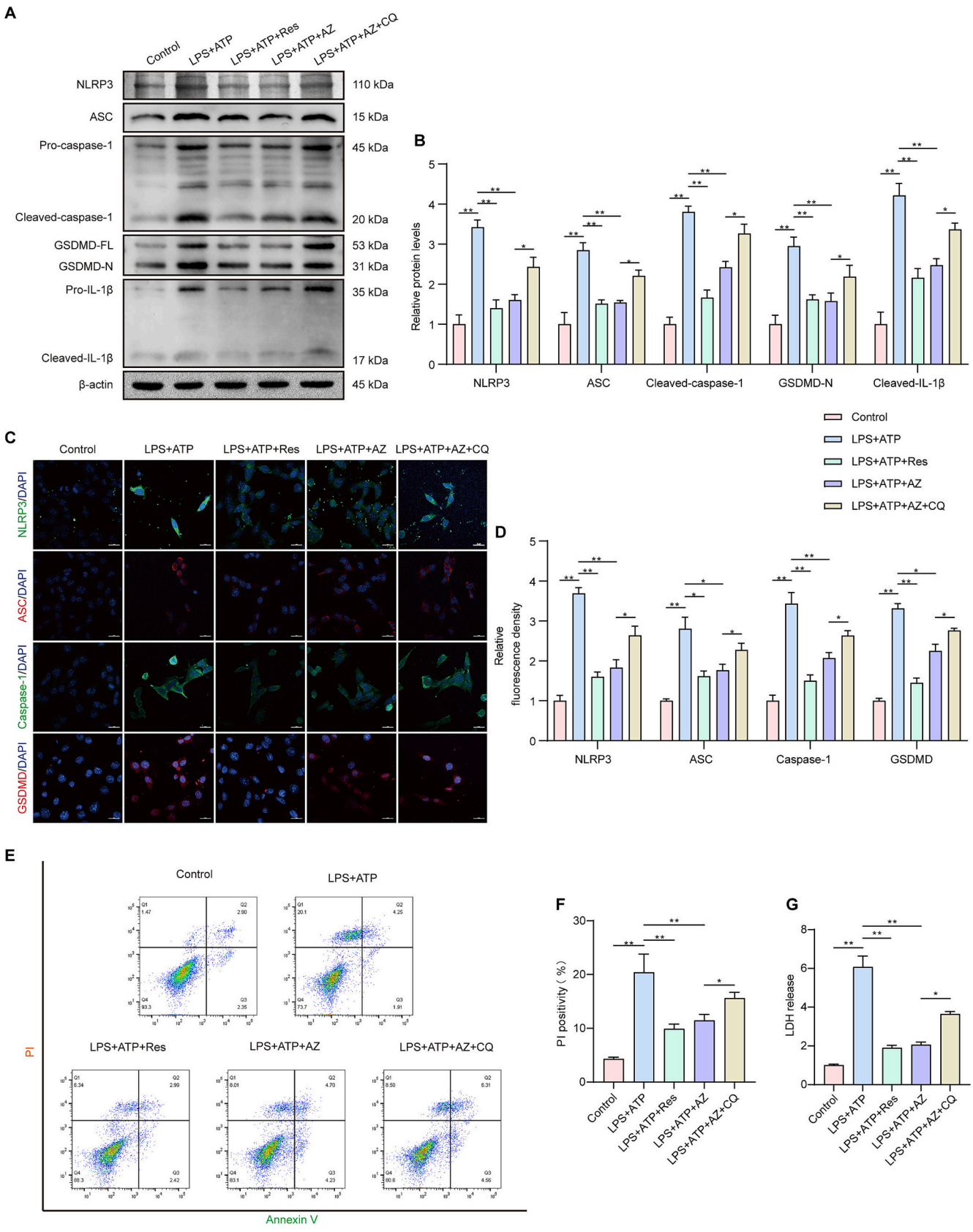

Fig. 5. AZ promotes mitophagy and suppresses pyroptosis in LPS-induced chondrocytes through the PINK1/Parkin signaling pathway. (A, B) Detection and quantification of NLRP3, ASC, Cleaved-caspase-1, GSDMD-N, and Cleaved-IL-1β protein expression by Western blotting and ImageJ analysis (n = 3). (C, D) Immunofluorescence images and quantitative analysis of NLRP3, ASC, Caspase-1, and GSDMD in chondrocytes of the indicated groups. Scale bar = 20 μm (n = 3). (E, F) Flow cytometric analysis and quantification of Annexin V-FITC/PI staining (n = 3). (G) LDH leakage assessed by ELISA assay in chondrocytes (n = 3). Data are expressed as mean ± SD. ns: not significant, $*p < 0.05$, and $**p < 0.01$, compared with the corresponding control.

down PINK1 in vitro. Western blot analysis revealed a marked reduction in PINK1 expression within the siPINK1 group, confirming the effective knockdown of PINK1 in chondrocytes (Supplementary Fig. 2 A, B). Notably, the LPS + ATP + AZ + siPINK1 group exhibited significantly lower levels of PINK1 and Parkin compared to the LPS + ATP + AZ + siNC group. Additionally, the expression of pyroptosis-related proteins NLRP3 and GSDMD was elevated in the LPS + ATP + AZ + siPINK1 group relative to the LPS + ATP + AZ + siNC group (Supplementary Fig. 2C, D). These findings indicate that PINK1 knockdown attenuates the ability of AZ to facilitate PINK1/Parkin-mediated mitophagy, thereby exacerbating chondrocyte pyroptosis. Therefore, based on these experimental results, we conclude that AZ inhibits LPS-induced chondrocyte pyroptosis by enhancing PINK1/Parkin-mediated mitophagy.

3.5. AZ inhibits LPS-induced ECM degradation in chondrocytes by promoting mitophagy

Degradation and loss of articular cartilage are major factors in the pathogenesis of OA. ECM synthesis-related proteins, such as Collagen II and aggrecan, while inhibiting catabolism-related proteins, including MMP-3 and MMP-13, is crucial for therapeutic intervention in OA [20]. To investigate the effect of AZ on LPS + ATP-induced ECM degradation in chondrocytes, we evaluated the expression levels of Collagen II, aggrecan, MMP-3, and MMP-13. Western blotting results indicated that both AZ and Res significantly increased the expression levels of Collagen II and aggrecan while effectively inhibiting the levels of MMP-3 and MMP-13 in LPS + ATP-treated chondrocytes (Fig. 6A, B). Conversely, CQ inhibited the protective effects of AZ, alleviating ECM degradation. Furthermore, the results of immunofluorescence and quantitative analysis of Collagen II, aggrecan, MMP-3, and MMP-13 in the treated cells were consistent with these findings, confirming the protective effect of AZ on chondrocyte ECM integrity (Fig. 6C, D). To further evaluate the efficacy of AZ in the treatment of osteoarthritis, rapamycin, a standard OA therapy, was used as a positive control. Western blot analysis revealed that both AZ and Rapa significantly reversed the LPS + ATP-induced reduction in collagen II and aggrecan protein expression, as well as the increase in MMP-3 and MMP-13 protein levels. No significant differences were observed between AZ and Rapa in their regulation of the extracellular matrix homeostasis (Supplementary Fig. 3 A, B). These results strongly suggest that AZ inhibits LPS-induced ECM degradation in chondrocytes by promoting mitophagy.

3.6. In vivo, AZ attenuates osteoarthritis progression by promoting mitophagy mediated by the PINK1/parkin signaling pathway and inhibiting chondrocytes pyroptosis

To further elucidate the mechanism of action of AZ on the progression of osteoarthritis, we randomized mice into four groups: sham, DMM, DMM + Res (50 mg/kg), and DMM + AZ (1 mg/kg). Micro-CT was employed to investigate whether AZ's protective effect on

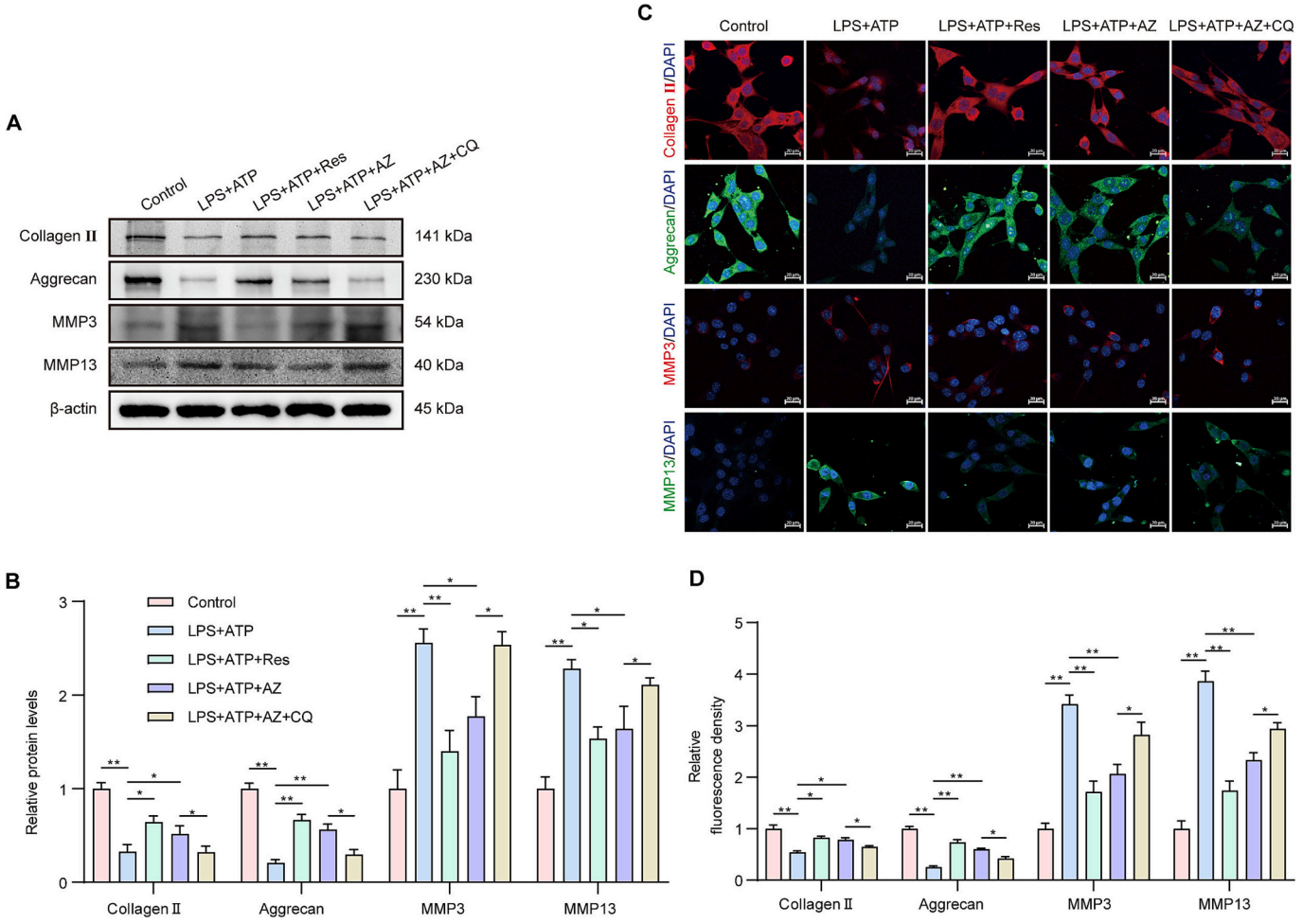

Fig. 6. AZ inhibits LPS-induced ECM degradation in chondrocytes by promoting mitophagy. (A, B) Detection and quantification of Collagen II, Aggrecan, MMP-3, and MMP-13 protein expression via Western blot and ImageJ analysis (n = 3). (C, D) Immunofluorescence images and quantitative analysis of Collagen II, Aggrecan, MMP-3, and MMP-13 in chondrocytes of the indicated groups. Scale bar = 20 μm (n = 3). Data are expressed as mean ± SD. ns, not significant; $*p < 0.05$, and $**p < 0.01$, compared with the corresponding control.

articular cartilage is associated with its potential impact on the subchondral bone microstructure of the tibia. The results revealed more calcified menisci and bone remnants in the DMM group compared to the sham group, with these abnormalities significantly reduced following treatment with AZ and Res (Fig. 7A). Bone and trabecular parameters of the subchondral bone of the tibia in mice showed that BV/TV and Tb.Th were decreased in the DMM group compared to the sham-operated group, while treatment with AZ and Res reversed these declines (Fig. 7B, C). The results of H&E and Safranin O/Fast Green staining indicated that DMM led to significant cartilage loss, depletion of proteoglycans, and elevated OARSI scores. Notably, these alterations were effectively attenuated by the administration of AZ and Res (Fig. 7D, E). These data suggest that AZ normalizes abnormal subchondral bone remodeling and inhibits osteochondral formation and cartilage damage in DMM mice. IHC further demonstrated that the expression of pyroptosis-related protein NLRP3 was significantly elevated in cartilage tissues of DMM group, while AZ and Res reversed these (Fig. 7F, G). Meanwhile AZ and Res significantly elevated Parkin and LC3B mitophagy-related protein expression in OA mouse tissues (Fig. 7F, G). Besides, AZ and Res reversed the decrease of Collagen II expression and the increase of MMP13 expression in OA tissues (Fig. 7F, G), which was consistent with the results of in vitro chondrocyte experiments. Collectively, these results suggest that AZ attenuates osteoarthritis progression by promoting mitophagy mediated by the PINK1/Parkin signaling pathway and inhibiting chondrocytes pyroptosis.

4. Discussion

Osteoarthritis (OA) is a major contributor to disability among the elderly population. Unfortunately, existing treatment options have shown limited efficacy in addressing cartilage degeneration, and there are currently no drugs approved specifically as disease modifiers for OA [44]. This gap in effective treatment underscores the urgent need for the development of new anti-OA drugs that can more effectively target the underlying mechanisms of the disease and promote cartilage health. Growing evidence suggests that mitochondria play a critical role in OA [45]. Previous studies have confirmed that an imbalance in mitophagy contributes significantly to mitochondrial dysfunction [46]. In OA, mitophagy is inhibited, leading to abnormal accumulation of functionally impaired mitochondria, which damages chondrocytes, and curcumin alleviates the progression of osteoarthritis by activating mitophagy through the AMPK/ PINK1/Parkin pathway [36]. The multifunctional properties of AZ stem from its unique chemical structure (3-[4-hydroxy-3-methoxybenzyl]pentane-2,4-dione), which contains the 4-hydroxy-3-methoxyphenyl ring found in both turmeric ketones and curcuminoids, as well as the 1,3- dicarbonyl group found only in curcuminoids, two potent natural skincare ingredients with antioxidant, anti-inflammatory and anti-aging properties [34]. Thus, the hybrid structure of AZ retains many properties of gingerone and curcumin, while also offering improved photochemical stability, particularly compared to curcumin, which degrades significantly under solar radiation. This stability makes AZ a promising candidate for the treatment of OA. In this study, validation experiments in chondrocytes and a mouse model demonstrated that AZ promotes mitophagy to inhibit chondrocyte pyroptosis via the PINK1/Parkin pathway, and alleviates OA pathology. These findings reveal a novel mechanism for AZ in preventing OA, highlighting its potential in OA treatment.

Inflammasome-mediated responses play a crucial role in host defense, but abnormal inflammasome regulation can contribute to autoimmune and aseptic inflammatory diseases [47]. The NLRP3 inflammasome is involved in cartilage degeneration and synovial inflammation by triggering the release of proinflammatory cytokines and degrading enzymes [48]. NLRP3 may serve as a potential biomarker for the management of OA [49]. Inhibition of NLRP3 inflammasome activity by Icariin or Cucurbitacin B reduces inflammatory cytokines and slows OA progression [16,50]. In the present study, AZ significantly inhibited NLRP3 inflammatory vesicle activation, cytokine release, and GSDMD-N formation in chondrocytes, suggesting that AZ could be a novel candidate for the treatment of NLRP3-driven diseases.

Mitochondrial damage increases mtROS production, which in turn leads to further mitochondrial damage and dysfunction, thus creating a "vicious cycle" that is associated with the development of OA [51,52]. Mitophagy is the phagocytosis of damaged mitochondria by double-membrane autophagosomes, which then fuse with lysosomes to form autolysosome, which are ultimately removed. This is part of cellular autophagy, which aims to degrade and remove damaged mitochondria to maintain normal cellular function and metabolic homeostasis [53]. Mitophagy plays a key role in reducing ROS production and preventing mitochondrial dysfunction, thereby enhancing chondrocyte activity [20,54]. When mitochondria are damaged, PINK1 rapidly accumulates at the mitochondrial membrane and recruits Parkin from the cytoplasm, which induces the degradation of the damaged mitochondria [55]. The results of this study indicate that AZ promotes the PINK1/Parkin-mediated mitophagy signaling pathway in chondrocytes. AZ significantly increased the expression of PINK1 and Parkin in both LPS-induced chondrocytes and DMM-induced mouse OA cartilage tissues, leading to a reduction in mitochondrial damage characterized by swelling, vacuolization, and structural incompleteness. Additionally, AZ treatment enhanced autophagic flux. Mitochondrial function assays demonstrated that AZ significantly reduced mtROS production and restored mitochondrial membrane potential, aligning with previous findings that activation of mitophagy improves mitochondrial function in OA [20,56]. These results suggest that AZ enhances mitophagy and improves mitochondrial structure and function in LPS-induced chondrocytes and DMM-induced cartilage tissues of mouse OA.

The mechanism by which organelle dysfunction contributes to NLRP3 inflammasome activation remains unclear [57]. Recent studies suggest that damaged mitochondria exhibit reduced membrane potential (MMP) and release ROS and mtDNA, both of which act as activators of NLRP3 inflammasome activation [58,59]. Mitochondrial dysfunction and ROS production promote the formation of NLRP3 inflammatory vesicles, leading to the oligomerization of GSDMD and the formation of pores in the cell membrane, ultimately resulting in pyroptosis [60,61]. Thus, impaired MMP and subsequent accumulation of ROS play a crucial role in the activation of NLRP3 inflammatory vesicles and pyroptosis in chondrocytes. Mitophagy-mediated degradation of damaged mitochondria can reduce NLRP3 activation [22,62]. We hypothesized that enhancing the elimination of damaged mitochondria could reduce NLRP3 activation and chondrocyte pyroptosis. Numerous studies have shown that Resveratrol attenuates toxicant-induced lung injury, kidney injury, and myocardial injury by promoting mitophagy through the PINK1/Parkin signaling pathway [42,43,63]. Our results show that AZ treatment attenuated mitochondrial damage and reduced ROS accumulation induced by impaired MMP. In contrast, inhibition of autophagy by the lysosomal inhibitor CQ reversed these effects, demonstrating that AZ regulates mitochondrial mass by promoting mitophagy and maintaining mitochondrial homeostasis. To assess whether AZ's effects on mitophagy and NLRP3 inflammatory vesicle activation are causal, we performed additional experiments. siPINK1 and CQ reversed the inhibitory effects of AZ on the expression of pyroptosis -associated proteins, including NLRP3, ASC, cleaved caspase-1, GSDMD-N, IL-1β, and LDH release. This suggests that AZ inhibits NLRP3 inflammatory vesicle activation by promoting mitophagy. Furthermore, both in vitro and in vivo experiments showed that AZ and Res promote the expression of mitophagy proteins Parkin and LC3B, inhibit the expression of the pyroptosis protein NLRP3, and alleviate chondrocyte pyroptosis. While their effects were similar, in vivo, AZ at a dose of 1 mg/kg was as effective as Res at 50 mg/kg, indicating AZ's significant therapeutic advantage in joint treatment. These findings suggest that AZ is a viable clinical candidate for targeting mitochondrial dysfunction and NLRP3 inflammasome activation, offering a promising therapeutic strategy for mitochondrial homeostasis and the regulation of

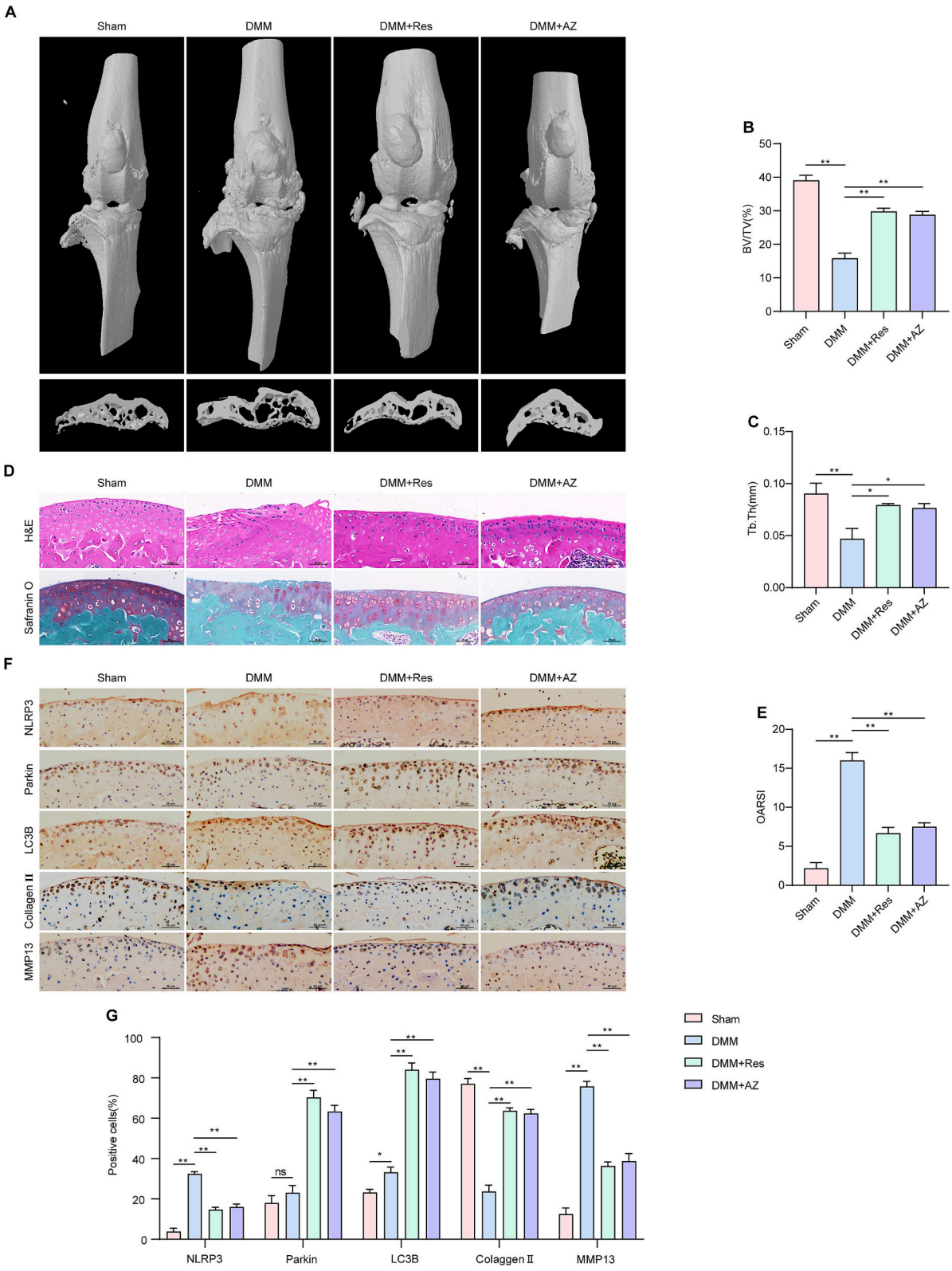

Fig. 7. AZ alleviates the progression of osteoarthritis in a mouse OA model. (A) Three-dimensional reconstruction of the mouse knee joint 4 weeks after surgery. Micro-CT image of sagittal views of the subchondral bone medial compartment 4 weeks after surgery. Scale bar = 9 μm. (B, C) Quantitative micro-CT analysis of the microarchitecture of the subchondral bone medial compartment, including bone volume/tissue volume (BV/TV, %) (B) and trabecular thickness (Tb.Th) (C). (D) H&E staining and safranin O/fast green staining were used to evaluate cartilage histopathology in OA mice. Cartilage damage (red arrow). Scale bar = 20 μm. (E) Osteoarthritis Research Society International (OARSI)-modified Mankin scores of articular cartilage at different time points after surgery. (F, G) Immunohistochemical staining and quantitative analysis of the expression of NLRP3, Parkin, LC3B, Collagen II, and MMP-13 in cartilage tissues. Data are expressed as mean ± SD. ns, not significant; $*p < 0.05$, and $**p < 0.01$, compared with the corresponding control. (For interpretation of the references to colour in this figure legend, the reader is referred to the web version of this article.)

pyroptosis in chondrocytes. AZ's therapeutic potential in the joints positions it as a strong contender for clinical application, with the ability to modulate intrinsic signaling pathways to regulate NLRP3 inflammatory vesicle activation and pyroptosis.

Articular cartilage is an avascular tissue composed of chondrocytes and extracellular matrix [64]. With the onset and progression of OA, chondrocyte proliferation and extracellular matrix synthesis gradually decrease, while chondrocyte apoptosis and matrix degradation increase [65]. Increasingly, studies have shown that inhibition of MMP3 and MMP13 production can halt the progression of OA [66]. IL-1β was found to cause significant downregulation of key components of the articular cartilage matrix, including Collagen II and Aggrecan, as well as upregulation of matrix metalloproteinases, including MMP3 and MMP-13 [7]. In contrast, activation of inflammatory vesicles with NLRP3 promotes the cleavage of Pro-IL-1β to mature Cleaved-IL-1β, releasing large amounts of pro-inflammatory cytokines [12]. Animal and cellular studies demonstrated that AZ reduced the expression of cleaved IL-1β, MMP-3, and MMP-13, while promoting the expression of collagen II and aggrecan. Furthermore, AZ exhibited similar extracellular matrix-modulating and osteoarthritis-relieving effects to the standard OA therapeutic agent rapamycin. These findings provide further evidence that AZ is a promising clinical candidate for the treatment of osteoarthritis.

Despite these significant findings, there are still research gaps to address. Future studies could focus on identifying the various signaling pathways that activate mitophagy in AZ. Biochemical and network pharmacology approaches could also be used to explore the mechanistic pathways, and techniques like immunoprecipitation and amino acid site mutation could help elucidate the interaction between AZ and its target proteins. These efforts will further clarify the mechanism underlying AZ's anti-OA effects. In summary, we found that AZ promotes mitophagy, inhibits LPS + ATP-induced chondrocytes pyroptosis and ECM degradation through the PINK1/Parkin signaling pathway, and slows down the progression of OA in a mouse model. Therefore, AZ presents a promising new therapeutic option for OA, offering a novel direction for clinical research and treatment.

CRediT authorship contribution statement

Zhuangzhuang Zhang: Writing – review & editing, Writing – original draft, Software, Methodology, Investigation, Formal analysis, Data curation. **Tianyue Huang:** Writing – review & editing, Writing – original draft, Software, Methodology, Investigation, Formal analysis. **Xu Chen:** Methodology, Formal analysis. **Jie Chen:** Writing – review & editing, Investigation. **Hang Yuan:** Writing – review & editing, Investigation. **Ning Yi:** Writing – review & editing, Investigation. **Chunbao Miao:** Writing – review & editing, Investigation. **Rongbin Sun:** Writing – review & editing, Supervision, Project administration. **Su Ni:** Writing – review & editing, Supervision, Project administration, Funding acquisition.

Funding

This study was supported by the Changzhou Science and Technology Program (CJ20245025 to N.S.); The Changzhou High-Level Medical Talents Training Project (2022CZBJ078 to N.S.); The Changzhou Health Commission Major Science and Technology Project (ZD202218 to N.S.).

Declaration of competing interest

The authors declare that they have no known competing financial interests or personal relationships that could have appeared to influence the work reported in this paper.

Acknowledgements

The all authors wish to thank the experimental platform provided by The Third Affiliated Hospital of Nanjing Medical University. Thanks to Figdraw for providing the graphical abstract drawing website.

Appendix A. Supplementary data

Supplementary data to this article can be found online at https://doi.org/10.1016/j.intimp.2025.115055.

Data availability

Data will be made available on request.

References

[1] G. Zhong, H. Long, S. Ma, Y. Shunhan, J. Li, J. Yao, miRNA-335-5p relieves chondrocyte inflammation by activating autophagy in osteoarthritis, Life Sci. 226 (2019) 164–172, https://doi.org/10.1016/j.lfs.2019.03.071.
[2] J. Martel-Pelletier, A.J. Barr, F.M. Cicuttini, P.G. Conaghan, C. Cooper, M. B. Goldring, et al., Osteoarthritis, Nat. Rev. Dis. Primers 2 (2016) 16072, https://doi.org/10.1038/nrdp.2016.72.
[3] Q. He, Y. Lin, B. Chen, C. Chen, J. Zeng, X. Dou, et al., Vitamin K2 ameliorates osteoarthritis by suppressing ferroptosis and extracellular matrix degradation through activation GPX4's dual functions, Biomed. Pharmacother. 175 (2024) 116697, https://doi.org/10.1016/j.biopha.2024.116697.
[4] B. Abramoff, F.E. Caldera, Osteoarthritis: pathology, diagnosis, and treatment options, Med. Clin. North Am. 104 (2) (2020) 293–311, https://doi.org/10.1016/j.mcna.2019.10.007.
[5] Y. D'Arcy, P. Mantyh, T. Yaksh, S. Donevan, J. Hall, M. Sadrarhami, et al., Treating osteoarthritis pain: mechanisms of action of acetaminophen, nonsteroidal anti-inflammatory drugs, opioids, and nerve growth factor antibodies, Postgrad. Med. 133 (8) (2021) 879–894, https://doi.org/10.1080/00325481.2021.1949199.
[6] Z. Lin, J. Zheng, M. Chen, J. Chen, J. Lin, The efficacy and safety of Chinese herbal medicine in the treatment of knee osteoarthritis: An updated systematic review and Meta-analysis of 56 randomized controlled trials, Oxidative Med. Cell. Longev. 2022 (2022) 6887988, https://doi.org/10.1155/2022/6887988.
[7] X. Kong, C. Ning, Z. Liang, C. Yang, Y. Wu, Y. Li, et al., Koumine inhibits IL-1β-induced chondrocyte inflammation and ameliorates extracellular matrix degradation in osteoarthritic cartilage through activation of PINK1/parkin-mediated mitochondrial autophagy, Biomed. Pharmacother. 173 (2024) 116273, https://doi.org/10.1016/j.biopha.2024.116273.
[8] Z. Rao, Y. Zhu, P. Yang, Z. Chen, Y. Xia, C. Qiao, et al., Pyroptosis in inflammatory diseases and cancer, Theranostics 12 (9) (2022) 4310–4329, https://doi.org/10.7150/thno.71086.
[9] X. Chen, G. Liu, Y. Yuan, G. Wu, S. Wang, L. Yuan, NEK7 interacts with NLRP3 to modulate the pyroptosis in inflammatory bowel disease via NF-κB signaling, Cell Death Dis. 10 (12) (2019) 906, https://doi.org/10.1038/s41419-019-2157-1.
[10] P. Huang, Z. Zhang, P. Zhang, J. Feng, J. Xie, Y. Zheng, et al., TREM2 deficiency aggravates NLRP3 inflammasome activation and Pyroptosis in MPTP-induced Parkinson's disease mice and LPS-induced BV2 cells, Mol. Neurobiol. 61 (5) (2024) 2590–2605, https://doi.org/10.1007/s12035-023-03713-0.
[11] J. Liu, S. Jia, Y. Yang, L. Piao, Z. Wang, Z. Jin, et al., Exercise induced meteorin-like protects chondrocytes against inflammation and pyroptosis in osteoarthritis by inhibiting PI3K/Akt/NF-κB and NLRP3/caspase-1/GSDMD signaling, Biomed. Pharmacother. 158 (2023) 114118, https://doi.org/10.1016/j.biopha.2022.114118.
[12] N. Kelley, D. Jeltema, Y. Duan, Y. He, The NLRP3 inflammasome: An overview of mechanisms of activation and regulation, Int. J. Mol. Sci. 20 (13) (2019), https://doi.org/10.3390/ijms20133328.
[13] K. Zhao, R. An, Q. Xiang, G. Li, K. Wang, Y. Song, et al., Acid-sensing ion channels regulate nucleus pulposus cell inflammation and pyroptosis via the NLRP3 inflammasome in intervertebral disc degeneration, Cell Prolif. 54 (1) (2021) e12941, https://doi.org/10.1111/cpr.12941.
[14] W. Liu, A. Liu, X. Li, Z. Sun, Z. Sun, Y. Liu, et al., Dual-engineered cartilage-targeting extracellular vesicles derived from mesenchymal stem cells enhance osteoarthritis treatment via miR-223/NLRP3/pyroptosis axis: toward a precision therapy, Bioact Mater 30 (2023) 169–183, https://doi.org/10.1016/j.bioactmat.2023.06.012.
[15] N. Zhang, J. Zhang, Y. Yang, H. Shan, S. Hou, H. Fang, et al., A palmitoylation-depalmitoylation relay spatiotemporally controls GSDMD activation in pyroptosis, Nat. Cell Biol. 26 (5) (2024) 757–769, https://doi.org/10.1038/s41556-024-01397-9.
[16] C. Lou, Y. Fang, Y. Mei, W. Hu, L. Sun, C. Jin, et al., Cucurbitacin B attenuates osteoarthritis development by inhibiting NLRP3 inflammasome activation and pyroptosis through activating Nrf2/HO-1 pathway, Phytother. Res. 38 (7) (2024) 3352–3369, https://doi.org/10.1002/ptr.8209.
[17] P.H. Willems, R. Rossignol, C.E. Dieteren, M.P. Murphy, W.J. Koopman, Redox homeostasis and mitochondrial dynamics, Cell Metab. 22 (2) (2015) 207–218, https://doi.org/10.1016/j.cmet.2015.06.006.

[18] X. Wang, Z. Liu, P. Peng, Z. Gong, J. Huang, H. Peng, Astaxanthin attenuates osteoarthritis progression via inhibiting ferroptosis and regulating mitochondrial function in chondrocytes, Chem. Biol. Interact. 366 (2022) 110148, https://doi.org/10.1016/j.cbi.2022.110148.
[19] Y. Lu, Z. Li, S. Zhang, T. Zhang, Y. Liu, L. Zhang, Cellular mitophagy: mechanism, roles in diseases and small molecule pharmacological regulation, Theranostics 13 (2) (2023) 736–766, https://doi.org/10.7150/thno.79876.
[20] L. Liu, W. Zhang, T. Liu, Y. Tan, C. Chen, J. Zhao, et al., The physiological metabolite α-ketoglutarate ameliorates osteoarthritis by regulating mitophagy and oxidative stress, Redox Biol. 62 (2023) 102663, https://doi.org/10.1016/j.redox.2023.102663.
[21] W. Li, Y. Zhong, Z. Lin, Z. Deng, D. Long, M. Li, et al., Forsythoside a mitigates osteoarthritis and inhibits chondrocyte senescence by promoting mitophagy and suppressing NLRP3 inflammasome via the Nrf2 pathway, Phytomedicine 135 (2024) 156052, https://doi.org/10.1016/j.phymed.2024.156052.
[22] Q. Lin, S. Li, N. Jiang, X. Shao, M. Zhang, H. Jin, et al., PINK1-parkin pathway of mitophagy protects against contrast-induced acute kidney injury via decreasing mitochondrial ROS and NLRP3 inflammasome activation, Redox Biol. 26 (2019) 101254, https://doi.org/10.1016/j.redox.2019.101254.
[23] X. Liu, M. Li, Z. Chen, Y. Yu, H. Shi, Y. Yu, et al., Mitochondrial calpain-1 activates NLRP3 inflammasome by cleaving ATP5A1 and inducing mitochondrial ROS in CVB3-induced myocarditis, Basic Res. Cardiol. 117 (1) (2022) 40, https://doi.org/10.1007/s00395-022-00948-1.
[24] F. Meng, C.A. Lowell, Lipopolysaccharide (LPS)-induced macrophage activation and signal transduction in the absence of Src-family kinases Hck, Fgr, and Lyn, J Exp Med. 185 (9) (1997) 1661–1670, https://doi.org/10.1084/jem.185.9.1661.
[25] P. Zhao, J. Ning, J. Huang, X. Huang, Mechanism of resveratrol on LPS/ATP-induced pyroptosis and inflammatory response in HT29 cells, Autoimmunity 57 (1) (2024) 2427094, https://doi.org/10.1080/08916934.2024.2427094.
[26] Y. Jin, H. Li, G. Xie, S. Chen, S. Wu, X. Fang, Sevoflurane combined with ATP activates caspase-1 and triggers caspase-1-dependent pyroptosis in murine J774 macrophages, Inflammation 36 (2) (2013) 330–336, https://doi.org/10.1007/s10753-012-9550-6.
[27] J. Shi, Y. Zhao, K. Wang, X. Shi, Y. Wang, H. Huang, et al., Cleavage of GSDMD by inflammatory caspases determines pyroptotic cell death, Nature 526 (7575) (2015) 660–665, https://doi.org/10.1038/nature15514.
[28] J. Qian, P. Fu, S. Li, X. Li, Y. Chen, Z. Lin, miR-107 affects cartilage matrix degradation in the pathogenesis of knee osteoarthritis by regulating caspase-1, J. Orthop. Surg. Res. 16 (1) (2021) 40, https://doi.org/10.1186/s13018-020-02121-7.
[29] J.W. Yu, M.S. Lee, Mitochondria and the NLRP3 inflammasome: physiological and pathological relevance, Arch. Pharm. Res. 39 (11) (2016) 1503–1518, https://doi.org/10.1007/s12272-016-0827-4.
[30] Z. Zhong, S. Liang, E. Sanchez-Lopez, F. He, S. Shalapour, X.J. Lin, et al., New mitochondrial DNA synthesis enables NLRP3 inflammasome activation, Nature 560 (7717) (2018) 198–203, https://doi.org/10.1038/s41586-018-0372-z.
[31] S.R. Mishra, K.K. Mahapatra, B.P. Behera, S. Patra, C.S. Bhol, D.P. Panigrahi, et al., Mitochondrial dysfunction as a driver of NLRP3 inflammasome activation and its modulation through mitophagy for potential therapeutics, Int. J. Biochem. Cell Biol. 136 (2021) 106013, https://doi.org/10.1016/j.biocel.2021.106013.
[32] W.R. Swindell, K. Bojanowski, R.K. Chaudhuri, A zingerone Analog, acetyl zingerone, bolsters Matrisome synthesis, inhibits matrix metallopeptidases, and represses IL-17A target gene expression, J. Invest. Dermatol. 140 (3) (2020) 602–614.e615, https://doi.org/10.1016/j.jid.2019.07.715.
[33] R.K. Chaudhuri, T. Meyer, S. Premi, D. Brash, Acetyl zingerone: An efficacious multifunctional ingredient for continued protection against ongoing DNA damage in melanocytes after sun exposure ends, Int. J. Cosmet. Sci. 42 (1) (2020) 36–45, https://doi.org/10.1111/ics.12582.
[34] T.A. Meyer, W.R. Swindell, R.K. Chaudhuri, Acetyl zingerone: a photostable multifunctional skincare ingredient that combats features of intrinsic and extrinsic skin aging, Antioxidants (Basel). 12 (6) (2023), https://doi.org/10.3390/antiox12061168.
[35] X. Chen, J. Chen, C. Miao, G. Yin, Z. Zhang, R. Sun, et al., Acetyl zingerone ameliorates osteoarthritis by inhibiting chondrocyte programmed cell death, Mol. Med. Rep. 28 (5) (2023), https://doi.org/10.3892/mmr.2023.13089.
[36] Z. Jin, B. Chang, Y. Wei, Y. Yang, H. Zhang, J. Liu, et al., Curcumin exerts chondroprotective effects against osteoarthritis by promoting AMPK/PINK1/parkin-mediated mitophagy, Biomed. Pharmacother. 151 (2022) 113092, https://doi.org/10.1016/j.biopha.2022.113092.
[37] S. Cao, C. Wang, J. Yan, X. Li, J. Wen, C. Hu, Curcumin ameliorates oxidative stress-induced intestinal barrier injury and mitochondrial damage by promoting parkin dependent mitophagy through AMPK-TFEB signal pathway, Free Radic. Biol. Med. 147 (2020) 8–22, https://doi.org/10.1016/j.freeradbiomed.2019.12.004.
[38] Y. He, Z. Wu, L. Xu, K. Xu, Z. Chen, J. Ran, et al., The role of SIRT3-mediated mitochondrial homeostasis in osteoarthritis, Cell. Mol. Life Sci. 77 (19) (2020) 3729–3743, https://doi.org/10.1007/s00018-020-03497-9.
[39] J.A. Bolduc, J.A. Collins, R.F. Loeser, Reactive oxygen species, aging and articular cartilage homeostasis, Free Radic. Biol. Med. 132 (2019) 73–82, https://doi.org/10.1016/j.freeradbiomed.2018.08.038.
[40] X. Yu, M. Hao, Y. Liu, X. Ma, W. Lin, Q. Xu, et al., Liraglutide ameliorates non-alcoholic steatohepatitis by inhibiting NLRP3 inflammasome and pyroptosis activation via mitophagy, Eur. J. Pharmacol. 864 (2019) 172715, https://doi.org/10.1016/j.ejphar.2019.172715.
[41] W. Fan, S. Chen, X. Wu, J. Zhu, J. Li, Resveratrol relieves gouty arthritis by promoting mitophagy to inhibit activation of NLRP3 inflammasomes, J. Inflamm. Res. 14 (2021) 3523–3536, https://doi.org/10.2147/jir.S320912.
[42] S. Liu, Y. Liu, J. Li, M. Wang, X. Chen, F. Gan, et al., Arsenic exposure-induced acute kidney injury by regulating SIRT1/PINK1/mitophagy Axis in mice and in HK-2 cells, J. Agric. Food Chem. 71 (42) (2023) 15809–15820, https://doi.org/10.1021/acs.jafc.3c05341.
[43] D. Wu, H. Zhang, F. Li, S. Liu, Y. Wang, Z. Zhang, et al., Resveratrol alleviates acute lung injury in mice by promoting Pink1/parkin-related mitophagy and inhibiting NLRP3 inflammasome activation, Biochim. Biophys. Acta Gen. Subj. 1868 (7) (2024) 130612, https://doi.org/10.1016/j.bbagen.2024.130612.
[44] L. Sharma, Osteoarthritis of the knee, N. Engl. J. Med. 384 (1) (2021) 51–59, https://doi.org/10.1056/NEJMcp1903768.
[45] K. Sun, X. Jing, J. Guo, X. Yao, F. Guo, Mitophagy in degenerative joint diseases, Autophagy 17 (9) (2021) 2082–2092, https://doi.org/10.1080/15548627.2020.1822097.
[46] M.Y.W. Ng, T. Wai, A. Simonsen, Quality control of the mitochondrion, Dev. Cell 56 (7) (2021) 881–905, https://doi.org/10.1016/j.devcel.2021.02.009.
[47] S. Christgen, T.D. Kanneganti, Inflammasomes and the fine line between defense and disease, Curr. Opin. Immunol. 62 (2020) 39–44, https://doi.org/10.1016/j.coi.2019.11.007.
[48] Y. Xiao, L. Zhang, Mechanistic and therapeutic insights into the function of NLRP3 inflammasome in sterile arthritis, Front. Immunol. 14 (2023) 1273174, https://doi.org/10.3389/fimmu.2023.1273174.
[49] M.J. McAllister, M. Chemaly, A.J. Eakin, D.S. Gibson, V.E. McGilligan, NLRP3 as a potentially novel biomarker for the management of osteoarthritis, Osteoarthr. Cartil. 26 (5) (2018) 612–619, https://doi.org/10.1016/j.joca.2018.02.901.
[50] Y. Zu, Y. Mu, Q. Li, S.T. Zhang, H.J. Yan, Icariin alleviates osteoarthritis by inhibiting NLRP3-mediated pyroptosis, J. Orthop. Surg. Res. 14 (1) (2019) 307, https://doi.org/10.1186/s13018-019-1307-6.
[51] D.B. Zorov, M. Juhaszova, S.J. Sollott, Mitochondrial reactive oxygen species (ROS) and ROS-induced ROS release, Physiol. Rev. 94 (3) (2014) 909–950, https://doi.org/10.1152/physrev.00026.2013.
[52] A. Hosseinzadeh, S.K. Kamrava, M.T. Joghataei, R. Darabi, A. Shakeri-Zadeh, M. Shahriari, et al., Apoptosis signaling pathways in osteoarthritis and possible protective role of melatonin, J. Pineal Res. 61 (4) (2016) 411–425, https://doi.org/10.1111/jpi.12362.
[53] S. Wang, H. Long, L. Hou, B. Feng, Z. Ma, Y. Wu, et al., The mitophagy pathway and its implications in human diseases, Signal Transduct. Target. Ther. 8 (1) (2023) 304, https://doi.org/10.1038/s41392-023-01503-7.
[54] Y. Shao, H. Zhang, H. Guan, C. Wu, W. Qi, L. Yang, et al., PDZK1 protects against mechanical overload-induced chondrocyte senescence and osteoarthritis by targeting mitochondrial function, Bone Res. 12 (1) (2024) 41, https://doi.org/10.1038/s41413-024-00344-6.
[55] D.P. Narendra, R.J. Youle, The role of PINK1-parkin in mitochondrial quality control, Nat. Cell Biol. 26 (10) (2024) 1639–1651, https://doi.org/10.1038/s41556-024-01513-9.
[56] D. D'Amico, M. Olmer, A.M. Fouassier, P. Valdés, P.A. Andreux, C. Rinsch, et al., Urolithin a improves mitochondrial health, reduces cartilage degeneration, and alleviates pain in osteoarthritis, Aging Cell 21 (8) (2022) e13662, https://doi.org/10.1111/acel.13662.
[57] P.I. Seoane, B. Lee, C. Hoyle, S. Yu, G. Lopez-Castejon, M. Lowe, et al., The NLRP3-inflammasome as a sensor of organelle dysfunction, J. Cell Biol. 219 (12) (2020), https://doi.org/10.1083/jcb.202006194.
[58] Y. An, H. Zhang, C. Wang, F. Jiao, H. Xu, X. Wang, et al., Activation of ROS/MAPKs/NF-κB/NLRP3 and inhibition of efferocytosis in osteoclast-mediated diabetic osteoporosis, FASEB J. 33 (11) (2019) 12515–12527, https://doi.org/10.1096/fj.201802805RR.
[59] H. Xian, K. Watari, E. Sanchez-Lopez, J. Offenberger, J. Onyuru, H. Sampath, et al., Oxidized DNA fragments exit mitochondria via mPTP- and VDAC-dependent channels to activate NLRP3 inflammasome and interferon signaling, Immunity 55 (8) (2022) 1370–1385.e1378, https://doi.org/10.1016/j.immuni.2022.06.007.
[60] C.L. Evavold, I. Hafner-Bratkovič, P. Devant, J.M. D'Andrea, E.M. Ngwa, E. Boršić, et al., Control of gasdermin D oligomerization and pyroptosis by the Ragulator-rag-mTORC1 pathway, Cell 184 (17) (2021) 4495–4511.e4419, https://doi.org/10.1016/j.cell.2021.06.028.
[61] T. Próchnicki, E. Latz, Inflammasomes on the crossroads of innate immune recognition and metabolic control, Cell Metab. 26 (1) (2017) 71–93, https://doi.org/10.1016/j.cmet.2017.06.018.
[62] X. Han, T. Xu, Q. Fang, H. Zhang, L. Yue, G. Hu, et al., Quercetin hinders microglial activation to alleviate neurotoxicity via the interplay between NLRP3 inflammasome and mitophagy, Redox Biol. 44 (2021) 102010, https://doi.org/10.1016/j.redox.2021.102010.
[63] Y. Liao, B. Ke, X. Long, J. Xu, Y. Wu, Abnormalities in the SIRT1-SIRT3 axis promote myocardial ischemia-reperfusion injury through ferroptosis caused by silencing the PINK1/parkin signaling pathway, BMC Cardiovasc. Disord. 23 (1) (2023) 582, https://doi.org/10.1186/s12872-023-03603-2.

[64] A. Bortoluzzi, F. Furini, C.A. Scirè, Osteoarthritis and its management - epidemiology, nutritional aspects and environmental factors, Autoimmun. Rev. 17 (11) (2018) 1097–1104, https://doi.org/10.1016/j.autrev.2018.06.002.
[65] Z. Yan, Z. He, H. Jiang, Y. Zhang, Y. Xu, Y. Zhang, TRPV4-mediated mitochondrial dysfunction induces pyroptosis and cartilage degradation in osteoarthritis via the Drp1-HK2 axis, Int. Immunopharmacol. 123 (2023) 110651, https://doi.org/10.1016/j.intimp.2023.110651.
[66] E.E. Mehana, A.F. Khafaga, S.S. El-Blehi, The role of matrix metalloproteinases in osteoarthritis pathogenesis: An updated review, Life Sci. 234 (2019) 116786, https://doi.org/10.1016/j.lfs.2019.116786.